Published by Avanti Publishers

Journal of Advances in Applied & Computational Mathematics

ISSN (online): 2409-5761

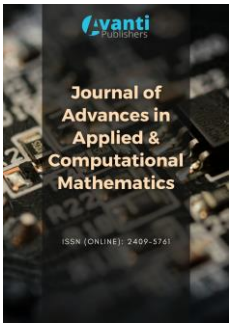

Optimization of Tuned Mass Damper for Submerged Floating Tunnel with Frequency-Domain Dynamics Simulation

Chungkuk Jin[1,*], Sung-Jae Kim[2] and MooHyun Kim[2]

[1]*Department of Ocean Engineering and Marine Sciences, Florida Institute of Technology, Melbourne, FL 32901, USA*
[2]*Department of Ocean Engineering, Texas A&M University, College Station, TX 77843, USA*

ARTICLE INFO

Article Type: Research Article

Keywords:
Optimization
Genetic algorithm
Tuned mass damper
Discrete module beam
Submerged floating tunnel

Timeline:
Received: August 11, 2022
Accepted: September 20, 2022
Published: October 20, 2022

Citation: Jin C, Kim S-J, Kim M. Optimization of tuned mass damper for submerged floating tunnel with frequency-domain dynamics simulation. J Adv App Comput Math. 2022; 9: 147-56.

DOI: https://doi.org/10.15377/2409-5761.2022.09.11

ABSTRACT

In this study, the Tuned Mass Damper (TMD) optimization is carried out to reduce the resonant motion of Submerged Floating Tunnel (SFT) under wave excitations. The SFT dynamics is evaluated in frequency domain; a new approach to cost-effectively optimizing TMD parameters for a moored system is suggested. Discrete-Module-Beam (DMB) method is used to model the Tunnel; mooring lines are included as equivalent stiffness matrix through static-offset tests by the fully coupled model. Since the frequency-domain dynamics simulation model is employed, a significant reduction in optimization time can be achieved. TMD is installed at the tunnel's mid-length to mitigate the lateral motion of the Tunnel and coupled with the Tunnel with translational and rotational springs and dampers. The optimization process for TMD parameters is performed through the Genetic Algorithm (GA). The GA generates the TMD mass and spring and damping coefficients. The dynamics simulation is performed under wave conditions and this process is repeated until the stopping criteria is satisfied. Results demonstrate that TMD with optimized parameters significantly reduces the lateral motion, especially near the system's lowest lateral natural frequency. This frequency-domain optimization also works as intended with significantly decreased optimization time.

*Corresponding Author
Email: cjin@fit.edu
Tel: +(1) 321 674 8934

1. Introduction

Submerged Floating Tunnel (SFT) has been proposed by researchers worldwide as a novel alternative to bridges, floating bridges, and immersed tunnels [1]. The SFT research is primarily due to its potential safety under various environmental loads if the design parameters are correctly selected, whereas other structures such as bridges, floating bridges, and immersed tunnels can be valuable to either ocean waves or submarine earthquakes [2]. Unfortunately, there is no actual construction in the world since many critical aspects are not fully understood and thus need to be studied thoroughly [3, 4].

One critical aspect is dynamic responses and mooring tensions under extreme wave and earthquake loads [5]. The dynamic motions and tensions are crucial concerns, especially for large-size SFTs—mooring lines can not handle large dynamic movements considering their commercially available maximum stiffness value, which may result in the system's failure. Snap loading is also prone to occur under large environmental loads, significantly increasing the mooring tension [6, 7]. Another critical aspect is the possibility of resonance under environmental loads at the target site. Changing the system's mass and stiffness is the simplest way to deal with resonance [8]. In the case of SFT, the system's natural frequency close to the target environmental loads can be avoided by modifying the Buoyancy-Weight Ratio (BWR) and mooring size/arrangement. However, considering that various environmental loads exist in the ocean, from low-frequency excitations such as tsunamis to high-frequency excitations such as ocean water waves and marine earthquakes, the simplest method may not work effectively. An alternative way is to install a vibration control device from passive to active control devices, as suggested by Ref. [9-13], for offshore structures. Among them, Tuned Mass Damper (TMD) is truly a proven device widely applied to many ocean structures, including SFT [13]. The TMD is connected to a main structure through springs and dampers. The TMD's natural frequency is tuned to the target frequency (e.g., the natural frequency of the main structure) so that TMD will resonate out of phase with the main structure. As a result, TMD dissipates the motion energy of the main structure induced by TMD's inertial force.

The TMD consists of mass, spring, and damper, and optimizing these parameters is one of the most critical tasks. For this mission, closed-form expressions were suggested for an undamped Single Degree Of Freedom (SDOF) system under harmonic and white noise excitations by Den Hartog [14] and Warburton [15]. However, it is well known that closed-form expression no longer exists when there is damping of the main structure and/or system shows nonlinear behaviors—the time-domain optimization method is inevitable for nonlinear systems [13, 16]. Then the optimization process is typically based on a numerical approach; representative examples include random decrement methods, metaheuristic algorithms, and machine learning [17-19]. In addition, various intelligent optimization methods can be employed for TMD optimization [20-23]. Another important consideration of TMD design is the system's elasticity, regarded as Multiple Degrees Of Freedom (MDOF) systems. In this case, TMD parameters are often correlated with mode shapes obtained by numerical simulation [24].

Since the SFTs showed nonlinear behaviors associated with mooring lines and had radiation/viscous damping components, time-domain optimization was often used [13, 25]. The biggest problem of time-domain optimization was enormous computation time. Since the optimization time was hugely associated with the simulation of the fully-coupled dynamics model in the time domain based on previous research, the simplified frequency-domain dynamics model is essential to reduce the computation time, which is proposed in this study.

This study develops the optimization method for TMD parameters inside SFT with the frequency-domain model. A passive TMD is modeled at the tunnel's mid-length to control lateral response. The hydro-elasticity of the tunnel is modeled by the Discrete-Module-Beam (DMB) method in frequency domain. The biggest concern of the frequency-domain analysis is the modeling of mooring lines. Mooring-line stiffness changes due to the TMD mass—the tunnel's vertical shape at a static state is changed by the TMD mass, which changes the equivalent stiffness of mooring lines associated with their static extension. For that, a static offset test at different TMD masses i.e., different static positions of the tunnel, is carried out to determine the equivalent stiffness. Then, the equivalent stiffness is obtained based on TMD mass at every iteration during the optimization process. Since the frequency-domain dynamics model cannot consider the nonlinear behavior of mooring lines, the tunnel's motion is assumed to be small. In addition, a Genetic Algorithm (GA) is chosen for the optimization process under wave excitations.

2. Configuration of Coupled System

The configuration of the tunnel and mooring lines are presented in Figure **1**. Key system parameters are summarized in Table **1**. The system consists of a tunnel and 52 mooring lines, and each mooring group is made up of four inclined mooring lines. One important note is that the tunnel's BWR is 1.1. In other words, the tunnel's buoyancy is 1.1 times larger than its dry weight, which is compensated by mooring lines. The TMD is located in the tunnel's geometric center and coupled with the main tunnel with springs and dampers.

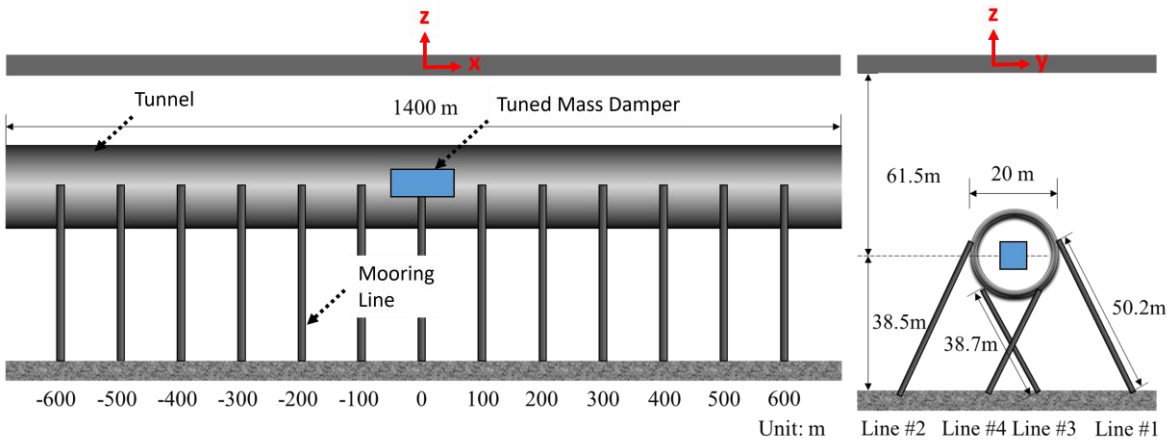

Figure 1: Design of tunnel, mooring lines, and TMD [13].

Table 1: Key design parameters for tunnel and mooring lines.

Component	Parameter	Value
Tunnel	Length Outer diameter End boundary condition Material Mass/unit length EA_c EI GJ BWR Added mass coefficient Drag coefficient	1400 m 20 m Fixed-fixed condition High-density concrete 292.7 t/m 4.9×10^9 kN 2.0×10^{11} kN·m^2 1.6×10^{11} kN·m^2 1.1 1.0 0.55
Mooring lines	Length Mass/unit length Nominal diameter EA_c EI Added mass coefficient Drag coefficient	50.2 m (Line# 1–2), 38.7 m (Line# 3–4) 0.64 t/m 0.18 m 2.77×10^6 kN 0 kN·m^2 1.0 2.4

*In the table, E and G are Young's modulus and shear modulus, A_c is the cross-sectional area, I is the lateral or vertical second moment of area, and J is the axial second moment of area.

3. Dynamics Simulation Model

3.1. Submerged Floating Tunnel Modeling in Frequency Domain

The DMB method is employed to model the hydro-elasticity of the tunnel. In this method, a very large floating structure is modeled with multiple rigid bodies and beam elements [26-28], as shown in Figure **2**. Since the details are described in Ref [29], only essential formulas are included in this paper. The frequency-domain equation of motion for M rigid bodies to model the tunnel can be expressed as:

$$\big(\boldsymbol{M}+\boldsymbol{A}(\omega)\big)\ddot{\boldsymbol{\xi}}+(\boldsymbol{B}(\omega)+\boldsymbol{B_R})\dot{\boldsymbol{\xi}}+(\boldsymbol{K_H}+\boldsymbol{K_M}+\boldsymbol{K_E})\boldsymbol{\xi}=\boldsymbol{F_W}(\omega) \tag{1}$$

where $\boldsymbol{M}$ is the mass matrix, $\boldsymbol{A}(\omega)$ and $\boldsymbol{B}(\omega)$ are the frequency-dependent added mass and radiation damping matrices with angular frequency ω, $\boldsymbol{B_R}$ is the structural damping matrix, $\boldsymbol{K_H}$, $\boldsymbol{K_M}$, and $\boldsymbol{K_E}$ are the stiffness matrices related to hydrostatic restoring coefficients, mooring lines, and beam elements, $\boldsymbol{F_W}(\omega)$ is the frequency-dependent wave-excitation-force vector, and $\boldsymbol{\xi}$ is the displacement vector. The upper dot stands for time derivative. In Eq (1), hydrodynamic coefficients and wave excitation forces are obtained by three-dimensional (3D) radiation/diffraction hydrodynamic analysis in which the Laplace equation is governing equation with the assumption of incompressible, irrotational, and inviscid flow.

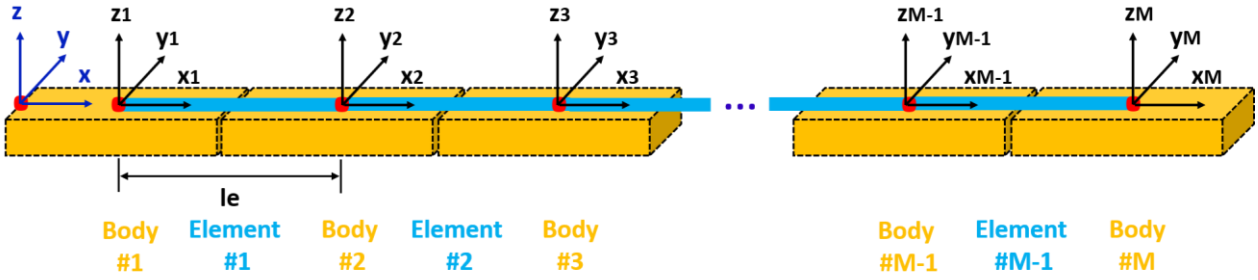

Figure 2: DMB method based on multiple rigid bodies and connecting high-order beams [29].

In Eq. (1), $\boldsymbol{K_E}$ is included to represent the elastic behavior of the tunnel. 12 by 12 sub-stiffness matrix $\boldsymbol{K}_e$ (i.e., one element between two neighboring rigid bodies) can be constructed by any beam theory; Euler-Bernoulli beam and Saint-Venant's torsion theory are employed to make $\boldsymbol{K}_e$ for the beam element number e in the local coordinate system, as in Eq. (2).

$$\boldsymbol{K}_e=\begin{bmatrix}
\frac{EA_c}{l_e} & & & & & & & & & & & \\
0 & \frac{12EI_z}{l_e^3} & & & & & & & & & & \\
0 & 0 & \frac{12EI_y}{l_e^3} & & & & & & & & & \\
0 & 0 & 0 & \frac{GI_x}{l_e} & & & & & & & & \\
0 & 0 & -\frac{6EI_y}{l_e^2} & 0 & \frac{4EI_y}{l_e} & & & & & & & \\
0 & \frac{6EI_z}{l_e^2} & 0 & 0 & 0 & \frac{4EI_z}{l_e} & & & & & & \\
-\frac{EA_c}{l_e} & 0 & 0 & 0 & 0 & 0 & \frac{EA_c}{l_e} & & & & & \\
0 & -\frac{12EI_z}{l_e^3} & 0 & 0 & 0 & -\frac{6EI_z}{l_e^2} & 0 & \frac{12EI_z}{l_e^3} & & & & \\
0 & 0 & -\frac{12EI_y}{l_e^3} & 0 & \frac{6EI_y}{l_e^2} & 0 & 0 & 0 & \frac{12EI_y}{l_e^3} & & & \\
0 & 0 & 0 & -\frac{GI_x}{l_e} & 0 & 0 & 0 & 0 & 0 & \frac{GI_x}{l_e} & & \\
0 & 0 & -\frac{6EI_y}{l_e^2} & 0 & \frac{2EI_y}{l_e} & 0 & 0 & 0 & \frac{6EI_y}{l_e^2} & 0 & \frac{4EI_y}{l_e} & \\
0 & \frac{6EI_z}{l_e^2} & 0 & 0 & 0 & \frac{2EI_z}{l_e} & 0 & -\frac{6EI_z}{l_e^2} & 0 & 0 & 0 & \frac{4EI_z}{l_e}
\end{bmatrix}_{symm.} \tag{2}$$

where E and G are Young's and shear moduli, A_c is the cross-sectional area, l_e is the element length, and I_x, I_y, and I_z are the torsional, vertical, and lateral second moments of area about x, y, and z axes, respectively. Then, $\boldsymbol{K_E}$ can be constructed for $M-1$ beam elements by properly overlapping $\boldsymbol{K}_e$ with the 6 by 6 sub-stiffness matrices of $\boldsymbol{K}_e$ as:

$$\boldsymbol{K}_E = \begin{bmatrix} \boldsymbol{K}_1^{(11)} & \boldsymbol{K}_1^{(12)} & 0 & \cdots & 0 \\ \boldsymbol{K}_1^{(21)} & \boldsymbol{K}_1^{(22)} + \boldsymbol{K}_2^{(11)} & \boldsymbol{K}_2^{(12)} & \cdots & 0 \\ 0 & \boldsymbol{K}_2^{(21)} & \boldsymbol{K}_2^{(22)} + \boldsymbol{K}_3^{(11)} & \cdots & 0 \\ \vdots & \vdots & \vdots & \ddots & \vdots \\ 0 & 0 & 0 & \cdots & \boldsymbol{K}_{M-1}^{(22)} \end{bmatrix} \tag{3}$$

$$\boldsymbol{K}_e = \begin{bmatrix} \boldsymbol{K}_e^{(ii)} & \boldsymbol{K}_e^{(ij)} \\ \boldsymbol{K}_e^{(ji)} & \boldsymbol{K}_e^{(jj)} \end{bmatrix}$$

3.2. Tuned Mass Damper Model

The Tuned Mass Damper (TMD) is located at the geometric center of the tunnel (i.e., the tunnel's center of gravity) for controlling lateral responses at the lowest lateral natural frequency. The TMD is modeled by the 6 DOF rigid body and translational/rotational springs/dampers. The TMD is coupled with the tunnel's mid-length by springs and dampers. It only allows relative lateral motion, while the other 5 DOF motions are synchronized between TMD and SFT. Synchronized movements can be achieved by having huge translational/rotational springs. Equation of motion given in Eq. (1) can be modified with the inclusion of TMD dynamics as:

$$\begin{bmatrix} \boldsymbol{M} + \boldsymbol{A}(\omega) & 0 \\ 0 & \boldsymbol{M_D} \end{bmatrix} \begin{Bmatrix} \ddot{\boldsymbol{\xi}} \\ \ddot{\boldsymbol{\xi}}_{\boldsymbol{D}} \end{Bmatrix} + \begin{bmatrix} \boldsymbol{B}(\omega) + \boldsymbol{B_R} + \boldsymbol{B_D} & -\boldsymbol{B_D} \\ -\boldsymbol{B_D} & \boldsymbol{B_D} \end{bmatrix} \begin{Bmatrix} \dot{\boldsymbol{\xi}} \\ \dot{\boldsymbol{\xi}}_{\boldsymbol{D}} \end{Bmatrix} + \begin{bmatrix} \boldsymbol{K_H} + \boldsymbol{K_M} + \boldsymbol{K_E} + \boldsymbol{K_D} & -\boldsymbol{K_D} \\ -\boldsymbol{K_D} & \boldsymbol{K_D} \end{bmatrix} \begin{Bmatrix} \boldsymbol{\xi} \\ \boldsymbol{\xi}_{\boldsymbol{D}} \end{Bmatrix} = \begin{Bmatrix} \boldsymbol{F_W}(\omega) \\ 0 \end{Bmatrix} \tag{4}$$

where a subscript $\boldsymbol{D}$ denotes TMD, and $\boldsymbol{B_D}$ and $\boldsymbol{K_D}$ are the damping and stiffness matrices for the SFT-TMD interaction.

3.3. Static Offset Test for Equivalent Mooring Stiffness

The $\boldsymbol{K_M}$ is obtained by a static offset test instead of modeling individual mooring lines. For the test, a tunnel-mooring-TMD fully-coupled dynamics model is used. In previous investigations, mooring stiffness can vastly be changed by its extension in the static condition, which results in the shift of natural frequencies. For instance, when the TMD mass increases in the optimization process, the static vertical location of the tunnel is lowered; static extension of mooring lines decreases; mooring stiffness decreases. The lumped-mass-method-based line model is used for this fully-coupled model to build the tunnel and mooring lines where a line consists of finite elements made of nodes and segments; physical properties and elastic deformations are considered in the nodes (lumped masses) and segments (massless axial, bending, and torsional springs). The details can be found in Ref. [30].

4. Optimization Process

The genetic algorithm (GA) is used in the optimization process inspired by biological evolution. Figure **3** shows the optimization process by GA. The algorithm starts from the random generation of a population of individuals (i.e., first-generation). After that, selection, crossover, and mutation are followed. Then a new generation is produced. The process is repeated until the stopping criteria satisfied. The highest-ranked evolved individual is considered the optimal combination of parameters. GA in MATLAB R2018a is used for this optimization. A large population size of 500 is selected to guarantee the performance in GA; the uniform random number generator

generates initial populations; the maximum number of generations and maximum stall generations are 300 and 100, respectively. Relatively large numbers compared to default values in GA are selected to avoid local minima and guarantee optimization performance.

The purpose of the TMD is to reduce tunnel motions. In previous investigations by authors [5, 6, 13, 25], lateral displacement was known to be critical to the SFT; thus, this study focuses on reducing lateral displacements through the TMD application. For each optimization, three simulations are conducted to guarantee the correctness of the obtained results. One of the simulation results is selected as the representative result in Section 5.

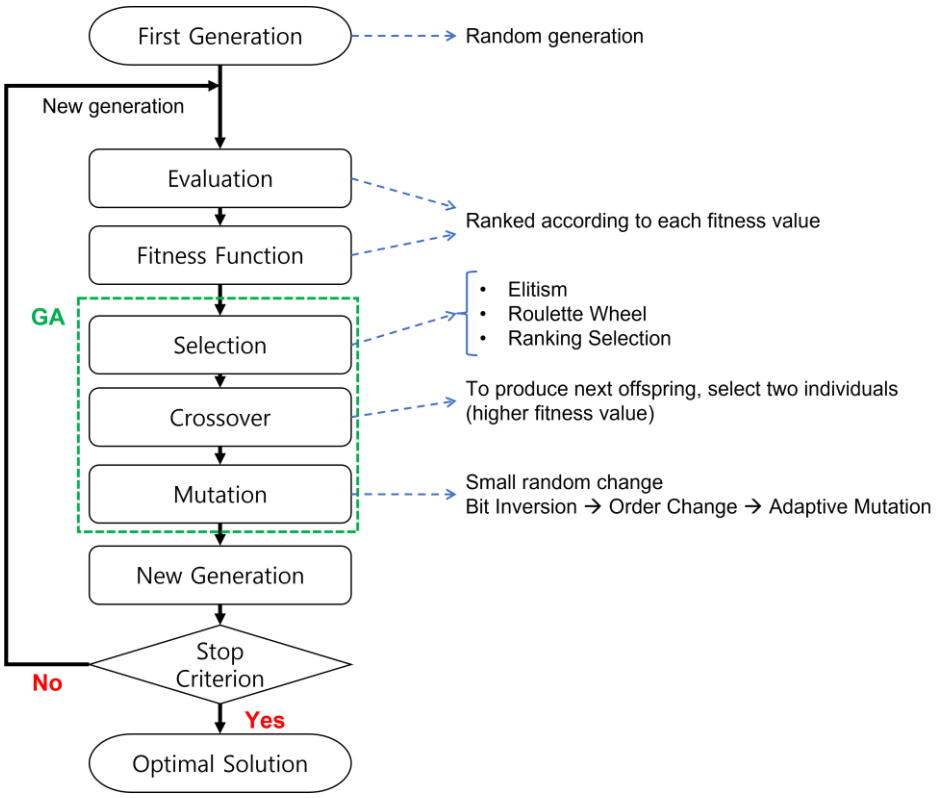

Figure 3: Optimization process by GA.

The TMD mass and spring/damping coefficients in the lateral direction are optimized in our case. At each simulation, the mass and spring/damping coefficients are produced by GA. Then the generated parameters are inputted to the dynamics simulation model described in Section 3. Before solving the equation of motion in Eq. (4), $\boldsymbol{K_M}$ is updated at the generated TMD mass through the static offset test. Then Eq. (4) is solved at each wave frequency, which leads to the Response Amplitude Operator (RAO). The JONSWAP wave spectrum $S_W(\omega)$ is considered a representative wave spectrum, which results in response spectrum calculation by $S_Y(\omega) = S_W(\omega)\left(RAO_Y(\omega)\right)^2$. The calculations of wave and response spectra are in the range of 0.02–2 rad/s with a 0.02 rad/s interval; the spectrum of lateral responses at the tunnel's mid-length is obtained; then, its standard deviation can be obtained, which is a square root of the spectral area. The standard deviation of the tunnel's lateral motion is the fitness function for GA—the lower the standard deviation, the better the TMD performance.

5. Results and Discussions

5.1. Validation of Frequency-Domain Dynamic Simulation Program

The Validation of the suggested dynamics simulation program is an essential task. This approach is based on frequency-domain formulations with mooring lines considered by the equivalent stiffness matrix instead of mooring lines modeled by Finite Element Method (FEM). Its validation can be obtained by comparing the present model with

the tunnel-mooring fully-coupled model. OrcaFlex, a commercial program, is used to model the fully-coupled model, and the detailed theory and methodology is provided by Refs. [5, 13, 31].

The Natural Frequencies and mode shapes are compared between the fully-coupled and present models, as presented in Table **2** and Figure **4**. This comparison does not consider TMD. Direct comparison of wet natural frequencies between two models is difficult since the current method uses frequency-dependent added mass while the fully-coupled model uses the Morison equation for added mass calculation. Thus, dry natural frequencies are only compared, as in Table **2**. Dry natural frequencies coincide between the programs. In addition, the dry mode shapes up to third modes in the lateral and vertical directions also support the correctness of the present model. In other words, inputting an equivalent stiffness matrix instead of complete modeling of mooring lines can be reasonable for this particular case. Of course, if the motion is too large, the present model may have errors in motion estimation since non-linear behaviors of mooring lines cannot be considered. Wet natural frequencies are also obtained by the present method, and frequency-dependent added mass and hydrostatic restoring co-efficient are additionally considered in wet natural frequency calculation. The results show that wet natural frequencies are lower than dry ones due to additional consideration of added mass/hydrostatic restoring co-efficient.

Table 2: Dry and wet natural frequencies of moored SFT up to 3 modes per direction (L and V denote lateral and vertical directions; the unit of natural frequencies in the table is rad/s).

	1st [L]	1st [V]	2nd [L]	2nd [V]	3rd [L]	3rd [V]
Fully coupled model (dry mode)	1.49	1.68	2.17	2.55	2.66	2.98
Present model (dry mode)	1.49	1.67	2.15	2.57	2.67	2.98
Present model (wet mode)	1.03	1.15	1.49	1.76	1.83	2.06

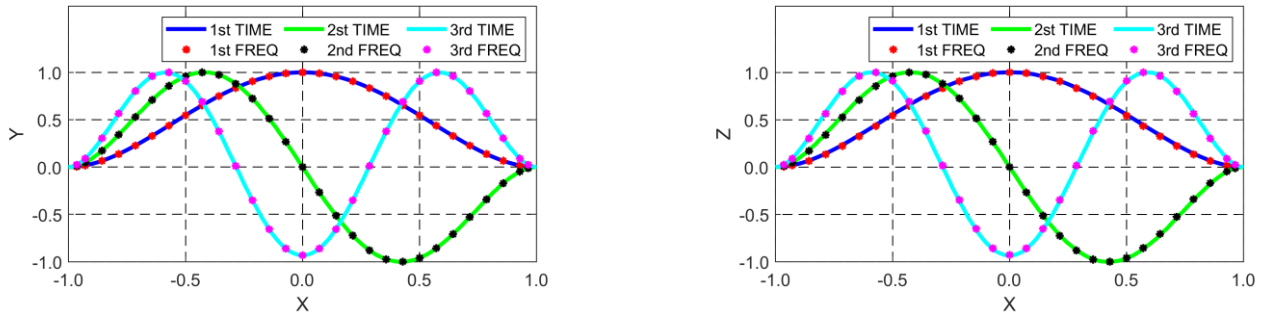

(a) Lateral direction

(b) Vertical direction

Figure 4: Normalized dry mode shapes between the fully-coupled time-domain SFT model and the present frequency-domain model (unit in the x- and y-axis is m/m).

5.2. Optimization of Tuned Mass Damper Parameters

The TMD mass and spring/damping coefficients are considered optimization parameters by GA. The maximum TMD mass is set at 2% of the modal mass at the lowest lateral natural frequency. The maximum spring and damping coefficients are 5000 kN/m and 1000 kNs/m. These maxima are considered practical/economic values for engineering practices [32, 33] and are set as the upper boundary in GA. Besides, lower limits for mass and spring/damping coefficients are set at 0.6% of the modal mass, 500 kN/m, and 100 kNs/m, respectively. Significant wave height and peak period are 3 m and 6 s, similar to the 100-yr storm condition in Norweigian Fjord. The enhancement parameter is set at 1.0 or 3.3.

Figure **5** shows response spectra of the tunnel's lateral motion with and without optimized TMD at its mid-length. Since the system's lowest lateral natural frequency without TMD is 1.03 rad/s and close to peak period of 6 s (= 1.05 rad/s), a substantial effect of TMD is observed regardless of the enhancement parameter value. The optimized mass and spring/damping coefficients at the enhancement parameter of 1.0 are 2415.3 t, 219.6 kNs/m, 2323.5 kN/m

(standard deviation = 1.24 cm), while they are 3818.6 t, 369.9 kNs/m, and 3669.0 kN/m (standard deviation = 1.26 cm) at the enhancement parameter of 3.3. The TMD's natural frequency at the enhancement parameter of 1.0 and 3.3 is 0.98 rad/s, which is close to the system's lowest lateral natural frequency of 1.03 rad/s without TMD, as presented in Table **2**. The resonance peak is distributed into two peaks, representing TMD's phenomenon.

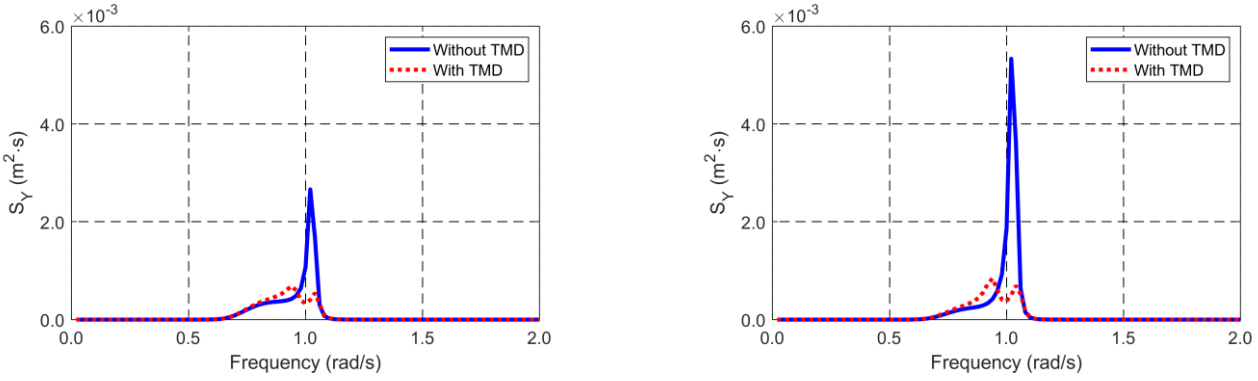

(a) Enhancement parameter = 1.0

(b) Enhancement parameter = 3.3

Figure 5: Response spectrum of tunnel's lateral motion with and without TMD at its mid-length and different enhancements parameters in the JONSWAP wave spectrum (Significant wave height of 3 m and peak period of 6 s).

To clarify the influence of the enhancement parameter on optimized values, optimization with respect to spring and damping coefficients is additionally conducted at eight different masses in the range of 0.6–2.0% of the modal mass. At each optimization, spring and damping coefficients are only optimized while the TMD mass is predefined.

Table **3** summarizes the optimized spring/damping coefficients and standard deviation values. As shown in Figure **6**, the larger the TMD mass, the lower the spectral energy until the resonant motion at 1.03 rad/s is almost mitigated. After that point, the performance decreases with increased TMD mass, which might be related to the change in mooring stiffness. Mooring stiffness is reduced as TMD mass increases associated with the static vertical location of the tunnel, which can increase the tunnel's lateral motion under wave excitations. Then, even though TMD performed well with larger mass, the standard deviation of the tunnel's lateral motion with TMD does not have a significant reduction or is even larger compared with one without TMD. Moreover, the TMD's operability is significantly reduced when the optimum spring coefficient reaches its upper boundary, such as with a TMD mass of 2.0%. Since optimum parameters vary due to the enhancement parameter, analyzing the site's environmental condition is of critical importance. Table **3** further supports these trends.

Table 3: Optimized spring/damping coefficients and standard deviation (STD) of tunnel's lateral response at different TMD masses.

Mass (t)	Mass (%)	Enhancement Parameter = 1.0			Enhancement Parameter = 3.3		
		Spring Coefficient (kN/m)	Damping Coefficient (kNs/m)	STD (cm)	Spring Coefficient (kN/m)	Damping Coefficient (kNs/m)	STD (cm)
Without TMD		-	-	1.47	-	-	1.79
2058.5	0.6	2008.5	172.4	1.25	2055.4	147.9	1.31
2744.7	0.8	2611.5	266.4	1.24	2701.2	227.3	1.28
3430.9	1.0	3177.6	371.2	1.25	3326.2	315.3	1.26
4117.2	1.2	3702.8	481.9	1.27	3925.4	414.5	1.27
4803.3	1.4	4182.0	591.9	1.31	4490.1	525.4	1.30
5489.4	1.6	4617.1	695.4	1.38	5000.0	650.8	1.35
6175.6	1.8	4979.6	791.8	1.50	5000.0	860.0	1.49
6861.8	2.0	5000.0	888.2	1.70	5000.0	1000.0	1.70

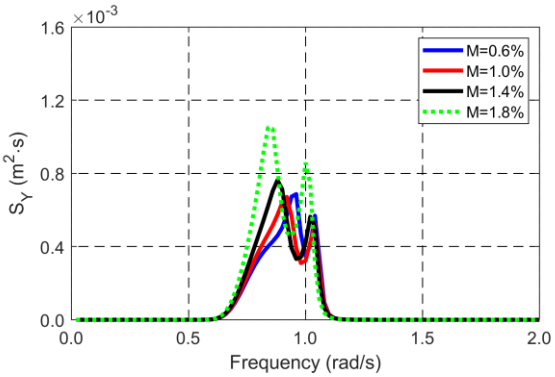

(a) Enhancement parameter = 1.0

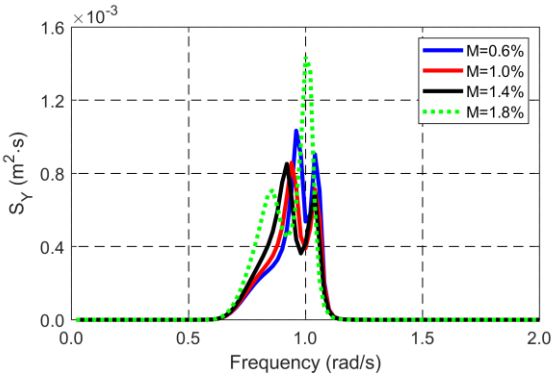

(b) Enhancement parameter = 3.3

Figure 6: Effects of TMD masses and environmental conditions (i.e., enhancement parameter in the JONSWAP wave spectrum) on response spectrum of tunnel's lateral motion with TMD at its mid-length.

6. Conclusions

This study presents the tuned mass damper (TMD) optimization for controlling the resonant motion of submerged floating tunnel (SFT) under wave excitations. The hydro-elasticity model with the discrete-module-beam method is first built to design the tunnel in frequency domain. The mooring lines are simplified with the equivalent stiffness matrix through a fully coupled model's static-offset test. The TMD is located at the tunnel's mid-length to control the lateral motion of the tunnel and is connected with the main tunnel with springs and dampers. Next, the optimization process is conducted through the genetic algorithm (GA). The GA produces the TMD mass and spring/damping coefficients. Then dynamics simulation with the JONSWAP wave spectrum is conducted with the generated TMD parameters. The GA continuously updates the parameter until the stopping criteria is satisfied. The performance of TMD is based on the standard deviation of the lateral motion of the tunnel at its mid-length.

Results show that significant resonant motion is largely reduced with the TMD, especially at the system's lowest lateral natural frequency. The optimized parameters are different with respect to the enhancement parameter. The higher the enhancement parameter, the higher the TMD parameters, which shows the importance of defining environmental conditions at a target site for TMD optimization.

References

[1] Jin C, Kim M, Chung WC, Kwon D-S. Time-domain coupled analysis of curved floating bridge under wind and wave excitations. Ocean Syst Eng. 2020; 10: 399-414.

[2] Jin C, Kim M-H. Tunnel-mooring-train coupled dynamic analysis for submerged floating tunnel under wave excitations. Appl Ocean Res. 2020; 94: 102008. https://doi.org/10.1016/j.apor.2019.102008

[3] Kim G-J, Kwak H-G, Jin C, Kang H, Chung W. Three-dimensional equivalent static analysis for design of submerged floating tunnel. Mar Struct. 2021; 80: 103080. https://doi.org/10.1016/j.marstruc.2021.103080

[4] Lee J, Jin C, Kim M. Dynamic response analysis of submerged floating tunnels by wave and seismic excitations. Ocean Syst Eng. 2017; 7: 1-19. https://doi.org/10.12989/ose.2017.7.1.001

[5] Jin C, Kim M. The effect of key design parameters on the global performance of submerged floating tunnel under target wave and earthquake excitations. CMES-Comput Model Eng Sci. 2021; 128: 315-37. https://doi.org/10.32604/cmes.2021.016494

[6] Jin C, Kim M-H. Time-domain hydro-elastic analysis of a SFT (submerged floating tunnel) with mooring lines under extreme wave and seismic excitations. Appl Sci. 2018; 8: 2386. https://doi.org/10.3390/app8122386

[7] Lu W, Ge F, Wang L, Wu X, Hong Y. On the slack phenomena and snap force in tethers of submerged floating tunnels under wave conditions. Mar Struct. 2011; 24: 358-76. https://doi.org/10.1016/j.marstruc.2011.05.003

[8] Yanik A, Aldemir U, Bakioglu M. Seismic vibration control of three-dimensional structures with a simple approach. J Vibrat Eng Technol. 2016; 4: 235-47.

[9] Wu Q, Zhao X, Zheng R, Minagawa K. High response performance of a tuned-mass damper for vibration suppression of offshore platform under earthquake loads. Shock Vibrat. 2016; 7383679: 1-11. https://doi.org/10.1155/2016/7383679

[10] Lee H, Wong S-H, Lee R-S. Response mitigation on the offshore floating platform system with tuned liquid column damper. Ocean Eng. 2006; 33: 1118-42. https://doi.org/10.1016/j.oceaneng.2005.06.008

[11] Wu B, Shi P, Wang Q, Guan X, Ou J. Performance of an offshore platform with MR dampers subjected to ice and earthquake. Struct Cont Health Monit. 2011; 18: 682-97. https://doi.org/10.1002/stc.398

[12] Zribi M, Almutairi N, Abdel-Rohman M, Terro M. Nonlinear and robust control schemes for offshore steel jacket platforms. Nonlinear Dyn. 2004; 35: 61-80. https://doi.org/10.1023/B:NODY.0000017499.49855.14

[13] Jin C, Chung WC, Kwon D-S, Kim M. Optimization of tuned mass damper for seismic control of submerged floating tunnel. Eng Struct. 2021; 241: 112460. https://doi.org/10.1016/j.engstruct.2021.112460

[14] Den Hartog JP. Mechanical vibrations. New York: Dover Publications 1985.

[15] Warburton G. Optimum absorber parameters for various combinations of response and excitation parameters. Earthquake Eng Struct Dyn. 1982; 10: 381-401. https://doi.org/10.1002/eqe.4290100304

[16] Bekdaş G, Nigdeli SM. Mass ratio factor for optimum tuned mass damper strategies. Int J Mechan Sci. 2013; 71: 68-84. https://doi.org/10.1016/j.ijmecsci.2013.03.014

[17] Lin C-C, Wang J-F, Ueng J-M. Vibration control identification of seismically excited mdof structure-PTMD systems. J Sound Vibrat. 2001; 240: 87-115. https://doi.org/10.1006/jsvi.2000.3188

[18] Bekdaş G, Nigdeli SM. Estimating optimum parameters of tuned mass dampers using harmony search. Eng Struct. 2011; 33: 2716-23. https://doi.org/10.1016/j.engstruct.2011.05.024

[19] Yucel M, Bekdaş G, Nigdeli SM, Sevgen S. Estimation of optimum tuned mass damper parameters via machine learning. J Build Eng. 2019; 26: 100847. https://doi.org/10.1016/j.jobe.2019.100847

[20] Ma L, Li N, Guo Y, Wang X, Yang S, Huang M, et al. Learning to optimize: reference vector reinforcement learning adaption to constrained many-objective optimization of industrial copper burdening system. IEEE Transact Cybernet. 2021; (e-pub ahead of print). https://doi.org/10.1109/TCYB.2021.3086501

[21] Ma L, Cheng S, Shi Y. Enhancing learning efficiency of brain-storm optimization via orthogonal learning design. IEEE Transact Syst Man, Cybernet Syst. 2020; 51: 6723-42. https://doi.org/10.1109/TSMC.2020.2963943

[22] Awad A, Hawash A, Abdalhaq B. A Genetic Algorithm (GA) and Swarm Based Binary Decision Diagram (BDD) Reordering Optimizer Reinforced with Recent Operators. IEEE Transact Evolut Comput. 2022; (e-pub ahead of print). https://doi.org/10.1109/TEVC.2022.3170212

[23] Alibrahim H, Ludwig SA. Hyperparameter optimization: comparing genetic algorithm against grid search and bayesian optimization. 2021 IEEE Congress Evolut Comput (CEC); 28 June 2021 - 01 July 2021; Kraków, Poland. IEEE: 2021; p. 1551-9. https://doi.org/10.1109/CEC45853.2021.9504761

[24] Sadek F, Mohraz B, Taylor AW, Chung RM. A method of estimating the parameters of tuned mass dampers for seismic applications. Earthquake Eng Struct Dyn. 1997; 26: 617-35. https://doi.org/10.1002/(SICI)1096-9845(199706)26:6<617::AID-EQE664>3.0.CO;2-Z

[25] Jin C, Kim S-J, Kim M. Vibration control of submerged floating tunnel in waves and earthquakes through tuned mass damper. Int J Naval Architect Ocean Eng. 2022; 14: 100483. https://doi.org/10.1016/j.ijnaoe.2022.100483

[26] Lu D, Fu S, Zhang X, Guo F, Gao Y. A method to estimate the hydroelastic behaviour of VLFS based on multi-rigid-body dynamics and beam bending. Ships Offshore Struct. 2016; 14: 354-62. https://doi.org/10.1080/17445302.2016.1186332

[27] Wei W, Fu S, Moan T, Lu Z, Deng S. A discrete-modules-based frequency domain hydroelasticity method for floating structures in inhomogeneous sea conditions. J Fluids Struct. 2017; 74: 321-39. https://doi.org/10.1016/j.jfluidstructs.2017.06.002

[28] Bakti FP, Jin C, Kim M-H. Practical approach of linear hydro-elasticity effect on vessel with forward speed in the frequency domain. J Fluids Struct. 2021; 101: 103204. https://doi.org/10.1016/j.jfluidstructs.2020.103204

[29] Jin C, Bakti FP, Kim M. Multi-floater-mooring coupled time-domain hydro-elastic analysis in regular and irregular waves. Appl Ocean Res. 2020; 101: 102276. https://doi.org/10.1016/j.apor.2020.102276

[30] Orcina. OrcaFlex User Manual Version 11.0 d. 2020.

[31] Jin C, Bakti FP, Kim M. Time-domain coupled dynamic simulation for SFT-mooring-train interaction in waves and earthquakes. Mar Struct. 2021; 75: 102883. https://doi.org/10.1016/j.marstruc.2020.102883

[32] Etedali S, Rakhshani H. Optimum design of tuned mass dampers using multi-objective cuckoo search for buildings under seismic excitations. Alexandria Eng J. 2018; 57: 3205-18. https://doi.org/10.1016/j.aej.2018.01.009

[33] Marano GC, Greco R, Trentadue F, Chiaia B. Constrained reliability-based optimization of linear tuned mass dampers for seismic control. Int J Solids Struct. 2007; 44: 7370-88. https://doi.org/10.1016/j.ijsolstr.2007.04.012